Indian Journal of Pure & Applied Physics
Vol. 62, November 2024, pp. 1029-1039
DOI: 10.56042/ijpap.v62i11.11409

Review Article

Review and modelling of Melting Point Depression in Metallic Nano Particles

Seema[a*], Sanjay Kashyap[b] & Chander Shekhar[a]

[a]Department of Applied Physics, Amity University, Haryana 122 413, India

[b]School of Physics & Materials Science, Thapar Institute of Engineering & Technology, Patiala, Punjab 147 004, India

Received 28 May 2024; accepted 19 September 2024

To improve the use of nanoparticles, it is imperative to comprehend the patterns and mechanisms driving their melting. The melting transformation thermodynamics has many formulas because of the phase equilibrium integrity and equilibrium presupposition of the different models. The analysis of the melting temperature depression for the nanoparticles has been done using a variety of melting models that have been published in the literature. These models include the following: Pawlow theory; Homogenous growth model; Heterogeneous growth model; Liquid nucleation & growth model; Liquid shell model; Homogenous melting and growth model; Bond order length strength model; Homogenous melting hypothesis; Liquid skin melting model; Reiss melting model and Rie melting model; Liquid drop model; Gibbs Thomson equation; Surface phonon instability model; and so on. In order to lower the melting point of the nanoparticles, this study reviews several melting models. The melting models align with the observed value of minute particles. Furthermore, the relationship between exact thermodynamic equations and their approximate counterparts is presented, as is the shift in melting temperature that occurs when nanoparticles melt.

Keywords: Size based melting; Melting temperature depression; Nanomaterials; Melting models

1 Introduction

Reduction in melting temperature refers to a drop in the melting point of constituents and compounds when their particle size decreases. While the melting point of bulk materials is constant with particle size, the melting point of nanomaterials (such as nanowire, nanoparticle, and nanotubes) varies with particle size. The melting point of nanomaterials may be hundreds of degrees lower than that of bulk materials in the case of nanoparticles. When compared to the bulk counterpart of the same material, the nanoparticles exhibit a significant variance in melting temperature due to their huge surface to volume ratio. There are numerous uses for the melting point depression of materials, including 1) material purity testing[1]. 2) To determine the thermal stability and phase relations in nanoparticles that differ from bulk materials. Additionally, a wide range of applications, including paints, filters, insulation, sensors, nano solders, and catalysts[2–7,] have made use of the understanding of melting point depression in nanoparticles. Because nanomaterials can be used for a wide range of purposes, it is required to compute the melting point reduction and particle melting process. The nanoparticles and bulk materials differ due to factors including phase relation, thermal stability, and high surface to volume ratio. For alloys and composites, melting is crucial because it influences processing and helps guarantee that the materials fulfil specifications for planned uses. It is critical to understand the metal's melting point since the alloying process needs to occur when the base metal is still liquid. A material's melting point can assist determine whether or not it is appropriate for a given application. For instance, a material with a higher melting point could be more costly to cast but more suited for machining. Instead of having a single melting point where a substance turns from solid to liquid, most alloys have a melting range. A substance is more impure the greater it's melting range. When an inhomogeneous composite structure is required, powder metallurgical techniques are employed to create the alloy rather than melting it.

Also, the discovery of polymeric materials including nanoparticles and their use in unique membranes has attracted growing interest. Polymers with incorporated nanoparticles show great promise in a number of sectors, such as electronics, healthcare, energy, and environmental science. High-performance materials and devices can be developed using nanoparticle-embedded polymers because of their special set of features. It has been noted that

*Corresponding author:
E-mail: seemasingroha91@gmail.com)

polymeric materials containing nanoparticles exhibit a broad range of functions, variable physicochemical properties, and a desirable compatibility with widely utilized membrane matrices. Nezar*et al*.[8] in this research, various fabrication processes including surface coating, self-assembly, interfacial polymerization, and phase inversion are explored and used to the production of homogenous nanoparticle-embedded polymeric materials and mixed-matrix membranes.

Ni/MgO@NCFs catalyst was successfully produced by loading varying weight percentages of Ni NPs (5, 10, and 15 wt%) supported on MgO-NCFs for active ammonia breakdown to create hydrogen that is carbon-free by Samikannu *et al*[9]. When compared to pristine NCFs, the Ni/MgO@NCFs (10 wt%) heterostructure showed increased catalytic activity towards ammonia breakdown at low temperatures. The heterostructure's increased surface area and transition metal are the causes of its increased catalytic activity. Given the vast array of applications for nanomaterials, it is imperative to compute the lowering of the melting point and comprehend the mechanism involved in the melting of nanoparticles. Due to the significantly different melting behaviors of nanoparticles compared to bulk materials, studies of the melting process and thermodynamic properties of nanoparticles have drawn interest from both theoretical and experimental perspectives. There are several experimental techniques available to ascertain the depletion in the melting temperature of nanoparticles, including Density Functional Theory (DFT) and Molecular Dynamics (MD).Melting temperature depression in a number of systems, such as carbon nanotubes, Nano spheres, and alumina Nano crystals, has been investigated using molecular dynamics simulations. Currently, molecular dynamics (MD) simulation and other computer simulation approaches have shown to be effective tools for studying the melting behavior of individual metal nanoparticles. In addition to offering sufficient and precise melting properties at the atomic level, MD can point the way toward a more extensive experimental examination of nanoparticles. The primary drawback of MD is its simulated time, which for big systems is currently in the order of nanoseconds. Numerous domains, including as material science, electronic materials, organic and inorganic chemistry, *etc*., use DFT. A quantum mechanical modeling technique called density functional theory (DFT) can be used to determine the electrical structure of atoms, molecules, and solids. Since DFT relies on fundamental principles, it may forecast material properties for unidentified systems without requiring experimental data. The current version of DFT has numerous drawbacks, including: too many approximations, failures for systems with strong correlations, too slowness for liquids, *etc*. Agglomeration of nanoparticles is a major problem that affects applications and measurement. Severe agglomeration of nanoparticles will lower the surface-to-volume ratio overall, which will lower or even eliminate the surface active characteristics. In comparison to a substance on a macroscopic size, the solid-to-liquid phase transition in nanoparticles is more intricate. Through rigorous theoretical research, the nature of the melting behaviour of nanoparticles can be discovered. With two-phase coexistence, several models suggest that the surfaces of nanoparticles melt at a lower temperature than the interiors. The melting behaviour of nanoparticles in various shapes can also be understood by modifying and applying thermodynamic models. The choice of a suitable melting model to predict and explain the melting behaviour of nanoparticles is still a critical problem for the continuous development of the melting transition thermodynamics of nanoparticles. The review of various melting models for the nanoparticles' melting point depression is presented in this work.

1.2 Measurement of Melting Point Depression

Because of their surface, nanomaterials have a significant impact on its properties. Solid surface atoms in nanomaterials have a lower cohesive energy than bulk atoms. Since an atom and all of its neighbours share chemical bonds, an atom with fewer bonds has less cohesive energy than an atom with fewer bonds. Equation[10] provides the standard formula for the size-dependent cohesive energy of the nanoparticles.

$$E_p = E_b \left(1-\frac{d}{D}\right) \quad \ldots(1)$$

Where-E_p, E_b, represent cohesive energy of the nanomaterials and the bulk materials, d and D are the grain size of the nanomaterials and the bulk respectively. The cohesive energy of the nanoparticles is reduced as the number of atoms at or near their surface is reduced. Lennard-Jones potential[11] states that an atom is drawn to other adjacent atoms due to an attractive force. Atomic cohesive and thermal energy are related to one another. The melting point of the materials is proportional to the cohesive energy (TM =

CaV), as demonstrated by Lindemann's Criterion[12,13]. Atoms close to the surface have fewer bonds and a lower cohesive energy. As a result, they need very little energy to separate an atom from a solid. When a nanoparticle's size is reduced, its surface atom count rises, leading to an increase in the particle's surface energy. As a result, compared to their bulk counterparts, the melting of the nanomaterials begins at a temperature that is significantly lower during the solid to liquid phase shift.

2 Thermodynamic Models for Nano Particle Melting

Numerous investigations have been conducted to simulate the decrease in melting point in relation to the particle size of the studied substance[14,15]. The present study provides a brief review of several thermodynamic models that have been reported in the literature, including Pawlow Theory, Liquid Drop Model, Liquid Shell Nucleation Model, Homogenous Growth Model, Heterogenous Growth Model, Liquid Nucleation and Growth Model, Homogenous Melting and Growth Model, Surface Phonon Instability Model, Gibbs Thomson Equation, Bond Order Length Strength Model, Homogenous Melting Hypothesis, Liquid Skin Melting, Reiss Melting Model, Rie Melting Model, and Semi-Empirical Model.

2.1 Pawlow Theory

Pawlow[14] modelled the melting temperature of the nanoparticles for the first time in 1909. As seen in Fig. 1, Pawlow proposed that equilibrium is established between the solid particle, micro droplet, and their saturated vapours throughout the melting process. Using Pawlow theory, the variation in the nanoparticle's melting point is provided below:

$$T_m = T_{mb}\left[1 - \frac{2}{rH_f}\left(\sigma_x^{solid}V_x^{solid} - \sigma_x^{liquid}\sigma_x^{liquid}\right)\right] \quad ...(2)$$

Where T_m,T_{mb},r, H_f, σ_x^{solid}, σ_x^{liquid},$V_x^{solid}$and V_x^{liquid} \are the melting temperature of nano and bulk particle, radius, heat of fusion, surface energy of component x in solid phase, surface energy of component x in liquid phase, molar volume of component x in the solid phase, molar volume of component x in the liquid phase respectively.

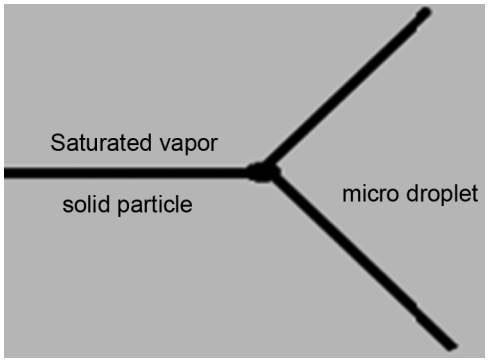

Fig.1 — The three-phase equilibrium between solid particles, saturated vapor, and micro droplets. According to Pawlow's idea, a nanoparticle's melting point is closely correlated with its reciprocal of size. Limitations of model are that the melting behaviour of many nanomaterials may be predicted using Pawlow theory, the theory does not work for nanoparticles with a radius of less than 5 nm[16]

2.2 Liquid Shell Nucleation (LSN) Model

Reiss and Wilson[17] presented this melting model in 1948. It is predicated on the equilibrium of a solid core with a thin liquid shell that forms on the core's surface, subsequently changed by A.R. Ubbelohde[18], who used a broad link between structural and thermodynamic changes that occur when a nanoparticle melts. Fig. 2 shows a schematic illustration of the nanoparticle melting process based on the liquid shell nucleation model. Subsequently, Hideki[19] computed the Pb nanoparticle's size-dependent melting point depression using Landau theory and the solid-liquid interface's width as a component. He discovered a non-linear relationship between the nanoparticle's radius and melting temperature. The melting behaviour of various nanoparticles, such as nanowires, nanofilms, and nanoparticles, is displayed by LSN. According to the LSN model, the surface layer of a nanoparticle melts initially because the surfaces of solids and liquids are in equilibrium. According to C. Q. Sun[20], the surface of a nanoparticle begins to melt first, resulting in a solid core with a liquid layer. This suggests that the liquid layer and the solid surface coexist until the

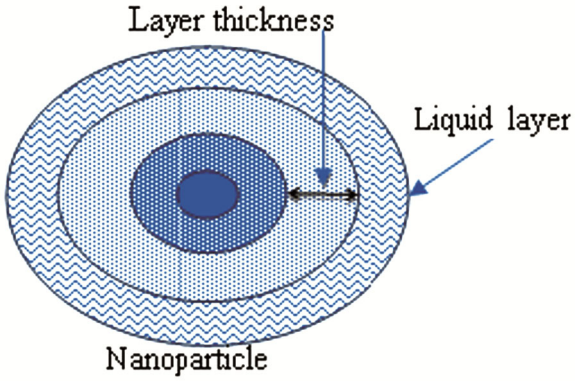

Fig. 2 — Schematic diagram of the melting of the nanoparticle based on the liquid shell nucleation model

solid core totally transforms into a liquid at the melting point.

This model attributes the radius of curvature of the nanomaterial to the melting temperature of the nanoparticles. Large-sized particles melt at greater temperatures. With the aid of this model, it has been possible to calculate the size and shape dependency of the melting of Sn, Au, and Al and to predict that the melting behaviour of Sn, Au, and Al dramatically decreases with the particle size. It has been noted that when the particle diameter reduces, the melting temperatures of Sn, Au, and Al also decrease. Landau potential was used to compute the melting condition in the LSN model. The variation in the nanoparticle's melting temperature based on these circumstances is shown below.

$$T_m = T_o \left[1 - \frac{2V_m(s)}{\Delta H} \left(\frac{\gamma_{sl}}{r-t} - \frac{\gamma_{lv}}{r} \left(1 - \frac{V_m(l)}{V_m(s)} \right)^{2/3} \right) \right] \quad ...(3)$$

Where, T_m, T_o, H_f, r, γ_{sl}, γ_{lv}, t, $V_m(l)$, and $V_m(s)$ is melting point of nanomaterial, bulk melting point,fusion heat of bulk particle, particle radius, solid-liquid interface energy of the bulk particle, liquid volume interface energy of bulk particles, the thickness of liquid layer and molar volume of the particle in liquid & solid-phase respectively.

The melting temperature remains unaffected when r>>t. As a result, the melting point of nanoparticles decreases with decreasing particle size, and melting happens layer by layer. The shortcoming of this model is that while the Landau theory has been used to analyse the size-dependence of melting temperature, the breadth of the solid-liquid interface has been overlooked. LSN model approaches the homogenous growth model when the liquid layer's thickness (t) is taken to be zero.

2.3 Homogenous Growth Model

The Gibbs Thomson equation was utilised by the Homogenous Growth Model (HOG)[21] to forecast the solid nanoparticle melting temperature. The HOG model accounts for variations in surface tension and volume (density). The melting point of a nanoparticle using the HOG approach is as follows:

$$T_m = T_o \left[1 - \Delta \frac{2V_m(s)}{\Delta H_f} (\sigma_{sv} - \sigma_{lv} \left(\frac{V_m(l)}{V_m(s)} \right)^{2/3}) \right] \quad ...(4)$$

Here T_m and T_o are nano and bulk melting temperatures, H_f is heat of fusion, $V_m(s)$ and $V_m(l)$ are molar volumes of bulk particles in the solid and liquid phase, σ_{sv} and $\sigma_{lv}$are the solid-vapor and liquid-vapor interface energy of the particle. Since HOG is a thermodynamic model, it can only provide the stability limit that is dependent on size. This model provides details on the melting process. Stated otherwise, it is expected that the particle undergoes instantaneous transformation at a given temperature, with minimal variation on temperature.

2.4 Heterogeneous Growth model

In 2007, Lee *et al*. proposed the Heterogeneous Growth (HEG) model, which assumes that the chemical potential of the liquid and solid phases is equivalent, i.e., $\mu(l) = \mu(s)$. The melting of nanoparticles depends on the heterogeneous development model (Fig. 3). This concept suggests that melting occurs at the interface between the particle and substrate as well as on the surface of the nanoparticle. Under different circumstances, the nanoparticle's shape and interface may alter while it lies on the substrate. Because of the surface and contact area with the substrate, the heterogeneous growth model differs in how it describes melting at the surface. Using the Heterogenous Growth Model, the effect of the substrates on the melting behaviour of Au nanoparticles with radii greater than 3 nm was computed[22]. It is observed that the melting point of the Au particle decreases with the reduction of particle size. The surface influences the particle and the contact between the particle and substrate simultaneously. The following represents the chemical potential of nanoparticles:

$$\mu(r) = \mu^{\infty} + \frac{C_1 V_m \Delta\gamma_{sv/lv}}{r} + \frac{C_2 V_m \Delta\gamma_{sc/lc}}{r} \quad ...(5)$$

Here C_1 and C_2 are the geometric factor used to describe the particle shape and interface area. V_m is molar volume, and r is the radius of nano particle.$\gamma_{sv/lv}$ and $\gamma_{sc/lc}$ are the interfacial energies of solid in equilibrium with liquid and vapor and carrier film respectively. Furthermore, C1 and C2 are

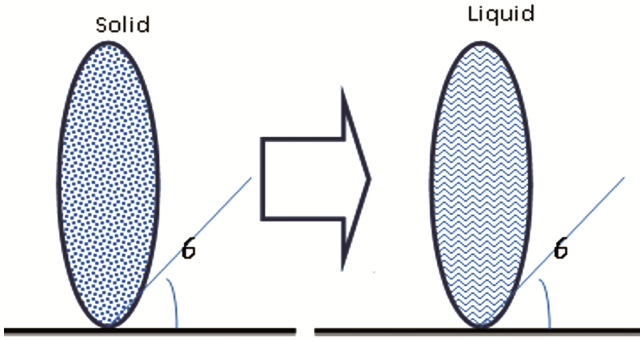

Fig. 3 — Nanoparticle melting on dependant upon Heterogeneous growth model

dependent on the contact angle θ, which is an important factor in shaping the nanoparticle's size-dependent characteristics. Because of the uneven contact between the nanoparticle and the substrate, the values of C1 and C2 drop. The contact angle is barely affected by the nanoparticle's melting temperature. The melting process in the HGM model is seen in Fig. 3.

2.5 Liquid Nucleation and Growth (LNG) Model

In 1977, Couchman and Jesser[23] presented the LNG Model. Subsequently, Reiss[24] and Richard et al[25] noted that the nucleation of liquid droplets on solid surfaces is the first step towards surface melting in the LNG model. The melting schematics provided by the liquid nucleation and growth model are shown in Fig. 4. The solid-liquid interface passes through the solid as it melts at the melting point. The free energy equilibrium condition varies in response to changes in the external environment, which encourages the melting of the nanoparticle. There is a finite activation energy associated with melting. At the interface, there is a zone where melting takes place as the particle alternates between solid and liquid phases. To put it simply, a rise in temperature causes a liquid layer to nucleate and expand in volume. Until the particle's dimension exceeds the critical radius, there is an energy barrier separating the liquid and solid phases. The remaining solid phase melts instantly when the nanoparticle dimension is smaller than the critical radius (core radius < critical radius). With a change in the particle radii, the melting temperature of nanoparticles is as follows:

$$T_m = T_o \left[1 - \frac{3}{\Delta H_o}\left(\frac{\gamma_{sl} V_m(s)}{r(s)} - \frac{\gamma_{lv} V_m(l)}{r(l)}\right)\right] \quad ...(6)$$

Here, T_m and T_o are nano and bulk melting point of particle, ΔH_o is heat of fusion, r(s) & r(l) is solid and liquid phase radius pf particle, $V_m(s)$ and $V_m(l)$ are molar volumes of bulk particle in the solid and liquid phase, γ_{sl} and γ_{lv} are solid-liquid and liquid-vapor interface energy of the bulk particle.

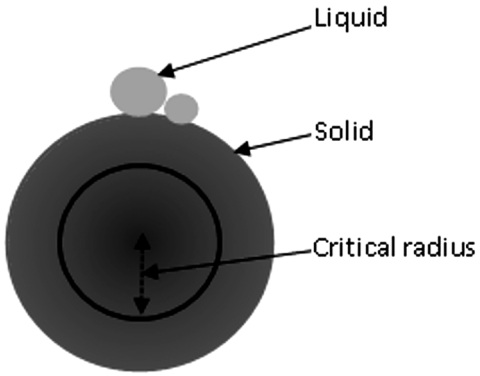

Fig. 4 — The schematics of the melting given by the liquid nucleation and growth model

2.6 Homogenous Melting and Growth (HMG) Model

Three mechanisms underpin the homogenous melting and growth model[26]:

(1) Instantaneous transformation in particle dimension.
(2) The solid state is eliminated.
(3) Differences in physical attributes.

Using the HMG melting model, the nanomaterials' melting point depression is as follows:

$$T_m = T_{mb}\left[1 - \frac{\sigma_{sv} - \sigma_{lv}}{d}\left(\frac{\rho_s}{\rho_l}\right)^{2/3}\right] \quad ...(7)$$

Here T_m,T_{mb}, σ_{sv}, σ_{lv}, ρ_s, ρ_l and d is melting temperature of nanomaterial, melting temperature of bulk, solid-vapor interface energy, liquid-vapor interface energy, density of the solid, density of the liquid and nanoparticle diameter respectively.

Gold nanoparticles have been used as the measuring medium for the HMG model. A decrease in the diameter of the gold nanoparticles has been seen, and this has been found to correlate well with the experimental evidence for low vapour pressure metals[26]. This model works better with larger particles (d>20 Å), since severe melting is not seen with particles smaller than 20 Å.

2.7 Bond Order Length Strength (BOLS) Model

Sun *et al*.[20,27,28] developed the BOLS model to characterise the melting temperature of the nanoparticle. The BOLS approach differs in that it is based on the cohesive strength of each individual atom and takes into account atomic considerations. The cohesive energy equilibration process[21] is used to compute the melting point of the nanomaterial, and the result indicates that: Heat capacity of the bulk and nano particles is similar.

(1) Nanoparticles have a bigger surface area than bulk material.
(2) The atomic radius naturally relaxes, or becomes calm.
(3) The cohesive energy of the particles with small grain sizes varies depending on bond strength and diatomic coordination number.
(4) A relaxed bond's binding energy rises.

Dimension dependent melting point of the nanomaterials based on BOLS model is given as:-

$$\frac{\Delta T_m}{T_{mb}} = -\sum \gamma_i \left(Z_{ib} C_i^{-m} - 1\right) \quad ...(8)$$

Here C_i^{-m}, $Z_{ib} = Z_i/Z_b$,γ_i, is the energy change of relaxed single bond,normalized coordination number, surface to volume ratio for nanomaterial respectively. Interatomic contact occurs close to the surface in this model, and surface area grows as particle diameter decreases. In comparison to its bulk equivalent, the BOLS model computes the surface layer of a nanoparticle melting at a lower temperature. The melting of the two outermost atomic layers and the atom that is still in the bulk predict the melting temperature of the nanoparticle. The BOLS model has been utilised to compute the size-dependent melting temperature of Au[23], Ni, Pd, and Pt[29]. A drop in the melting temperature of Au, Ni, Pd, and Pt has been observed as the particle size decreases. It is mostly caused by atomic cohesive energy because of the reduction in melting temperature. Another benefit of this model is that it only requires two parameters: the bulk particle's melting temperature and average bond distance. It also entails no assumptions or free adjustment variables.

2.8 Homogenous Melting Hypothesis (HMH)

The melting temperature of the nanomaterials is determined using this thermodynamic model, and the mathematical equation is provided as[30]. Diagrammatic representation of nanoparticle melting based on HMH in Fig. 5.

$$T_m = T_{mb}\left[1 - \frac{4V}{H_f d}\left\{\gamma_{sv} - \gamma_{lv}\left(\frac{\rho_s}{\rho_l}\right)^{2/3}\right\}\right] \quad ...(9)$$

Or $T_m = T_{mb}\left(1 - \frac{\beta}{d}\right)$

where $\beta = \frac{4V}{H_f}\left\{\gamma_{sv} - \gamma_{lv}\left(\frac{\rho_s}{\rho_l}\right)^{2/3}\right\}$

Here, T_m and T_{mb} are the melting temperatures of nano and bulk particle, V is the molar volume of the particle, d is the particle diameter, H_f is the heat of fusion of the particle, γ_{sv} and γ_{lv} are solid-liquid and liquid-vapor interface energy of the particle, and ρ_s and ρ_l are the solid and liquid density.

Using the HMH model, calculations of the Pb nanoparticles' melting point have been published. It has been determined that i) the Pb nanoparticle melting temperature decreases as the nanoparticle radius decreases. Regarding nanowires and nanofilms, the value of $\beta = \frac{4V}{H_f}\left\{\gamma_{sv} - \gamma_{lv}\left(\frac{\rho_s}{\rho_l}\right)^{2/3}\right\}$, is around 1.5, and ii) there is no surface melting and solid and liquid remain in equilibrium throughout the melting process.

2.9 Liquid Skin Melting

Another thermodynamic model that is useful for determining the melting temperature depression of nanoparticles is liquid skin melting[30]. Diagrammatic depiction of the liquid skin melting model in Fig. 6. Using this model, the size-dependent melting temperature of Sn nanoparticles has been found, and a decrease in the melting temperature is observed with a decrease in the size of the nanoparticles. According to

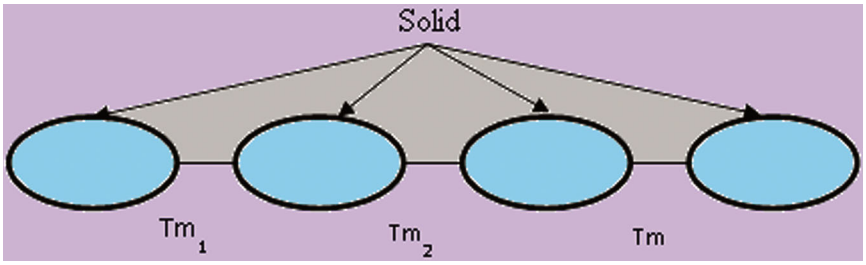

Fig. 5 — Schematic diagram representing the melting of nanoparticle-based on HMH

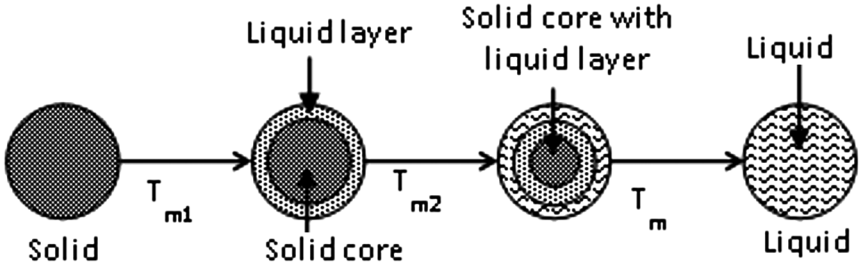

Fig. 6 — Schematic representation of liquid skin melting model

this idea, a liquid layer forms atop a solid at a lower temperature and stays there until the solid phase melts completely. The following is the description of the liquid skin melting model's mathematical expression:

$$T_m = T_{mb}\left(1 - \frac{4\gamma_{sl}V}{H_f(D-2\delta)}\right) \quad ...(10)$$

Here T_m,T_{mb} ,γ_{sl} ,V, H_f, D, and δ are the melting temperature of nano and bulk particles, solid-liquid interface energy, molar volume, the heat of fusion, nanoparticle diameter, and a constant respectively.Only the skin's melting layer is used to calculate the value of δ, which is always positive.

2.10 Reiss Melting Model

In 1948, Reiss and Wilson[31] and Curzon[32] presented the Reiss melting model to determine the melting point of low-grain-size nanoparticles. Fig. 7 shows a schematic depiction of the melting using the Riess melting model. The primary melting of nanoparticles can be explained using the Reiss melting model. The starting melting point represents the maximum melting point of the nanoparticles, and as the thickness of the liquid shell increases, the melting point decreases. The following is the mathematical expression for the Reiss melting model:

$$T_m = T_{mb}\left\{1 - \frac{2V_s}{\Delta_s H_m}\left[\frac{\sigma_{sl}}{r_1 - t} + \frac{\sigma_{lv}}{r_1}\left(1 - \frac{\rho_s}{\rho_l}\right)\right]\right\} \quad ...(11)$$

Here, T_m and T_{mb} are melting temperatures of nano and bulk particles, V_s is the molar volume of solid particle, $\Delta_s H_m$ is change in molar enthalpy of bulk phase at melting temperature, t is thickness of liquid layer, r_l is outside radius of liquid layer, r_s is radius of solid core, $\sigma_{sl,}$ and $\sigma_{lv}$are solid-liquid and liquid-vapor interface energy of particle, ρ_s and ρ_l are solid and liquid density of particle.

The Reiss model holds true for the basic melting step. Drawing the thickness of the liquid layer is necessary in order to determine the melting point of the nanomaterials. The melting temperature of a nanoparticle cannot be predicted by the Reiss melting model when the thickness of the liquid layer exceeds a critical amount.

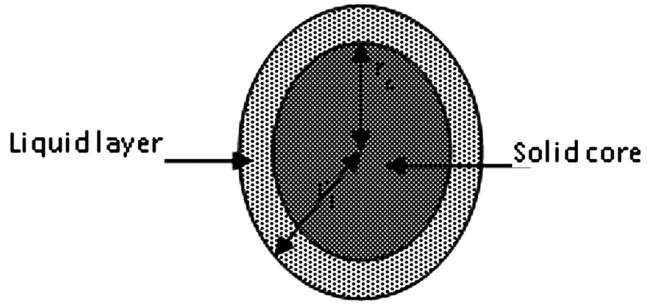

Fig.7 — Schematics representation of the melting as per Riess melting model

2.11 Rie melting Model

In 1923, Rie[33] put out the Rie model, which is a model for determining the melting point of nanomaterials. A liquid layer envelops solid particles during equilibrium melting, according to the Rie melting model. The following is the mathematical equation for the Rie melting model:

$$ln\frac{T_m}{T_{mb}} = \left(1 - \frac{2\sigma_{sl}V_s}{\Delta_s H_m r_s}\right)$$

consider $|T_m - T_{mb}| << T_{mb}$ then

$$\frac{T_m}{T_{mb}} = 1 - \frac{2\sigma_{sl}V_s}{\Delta_s H_m r_s} \quad ...(12)$$

Here T_m& T_{mb}, $\Delta_s H_m$, r_s, $V_{s,}$ and σ_{sl} represent melting temperatures of the nano and bulk particle,molar enthalpy change, radius of nano particle in the solid phase, molar volume, and solid-liquid interface energy of nano particle respectively. Using the Rie melting model, Jinhua et al.[29] calculated the Au nanoparticles' depression in melting temperature and came to the following conclusions: i) the Rie melting model is only applicable after the initial stage of melting; and ii) the melting temperature of the nanoparticles decreases as the particle radius decreases.

For a given material, the melting temperature determined by the Rie model is typically lower than the experimental measurement[34]. This disparity is greater for nanoparticles with r <5 nm. Additionally, a variety of models, including the liquid drop model[13], surface phonon instability model[35], Gibbs Thomson equation[36], and semi-empirical model[37], are available to compute the melting point depression of metals and compounds that have been described in the literature.

2.12 Liquid Drop Model

Nanda and Vanithakumari revised the Liquid Drop Model (LDM) to find the melting point of nanosolids. It establishes the connection between the cohesive energy, melting point, and surface tension of the materials. The melting point of nanoparticles[13] provides the cohesive energy of bulk particles per atom, which can be expressed as follows:

$$a_{v,d} = 0.0005736\, T_m$$

With a nano particle, the variation in cohesive energy per atom is given as-

$$a_{v,d} = a_v - \frac{6V_o\gamma}{d} \quad ...(13)$$

Here, the terms $a_{v,d}$,a_v,Vo, γ and d, respectively, stand for bulk cohesive energy per atom, bulk cohesive energy per coordination, the atomic volume of the nanoparticle, surface tension of the nanomaterials, and nanoparticle diameter. When expressed in terms of melting temperature, the following formula is provided for bulk cohesive energy per coordination (a_v):

$$a_v = 0.0005736\, T_{mb} + C \quad ...(14)$$

where C is a constant known as the straight line intercept and Tmb is the temperature at which bulk materials melt. The melting point of nanoparticles is represented by the following equations:

$$T_m = T_{mb} - \frac{6V_o\gamma}{0.0005736d}$$

$$T_m = T_{mb}\left(1 - \frac{6V_o\gamma}{0.0005736d\, T_{mb}}\right) \quad ...(15)$$

The inability of the LDM model to explain the pairing idea and its nuclear features is one of its drawbacks. This strategy does not allow us to foresee how the nuclei of lighter elements will be understood.

2.13 Gibbs Thomson Equation

The melting point of the nanoparticle is expected to drop if the liquid and crystal are in equilibrium and the liquid melts at a lower temperature than the bulk crystal, according to the Gibbs Thomson equation[36]. The Gibbs Thomson formula is as follows:

$$T_m = T_{mb}\left(1 - \frac{4\sigma_{sl}}{\rho_s H_f d}\right) \quad ...(16)$$

Here- T_m is nano melting temperature, T_{mb} is bulk melting temperature,σ_{sl} is solid liquid interface energy, d isdiameter of nano materials, H_f is latent heat of fusion and ρ_s is solid density of particle.According to this method, a rise in surface tension corresponds to a decrease in radius. The Gibbs-Thomson equation can only be applied when there is not an unduly big melting point depression of the nanomaterials.

2.14 Semi-Emprical Model

A semi-empirical model[38] is used to calculate the melting temperature of the nano solid based on dimensions (nanoparticle, nano wire, nano film).This is how a semi-empirical model is defined:

$$T_m = T_o\left(1 - \frac{N}{2n}\right) \quad ...(17)$$

Where T_m; melting point of nano particle, T_o; bulk melting point, N ; number of a surface atom of the solid, n ; total number of atom of the solid.

Melting temperature of the nano particle depends upon $\frac{N}{2n}$ which depend further on size and shape of the nano particle. Melting temperature of the nano particlesis the function of size and needed parameter are bulk melting point and atomic diameter.$\frac{N}{n}$ value for spherical particle[39] is $\frac{4d}{D}$ where d and D are atomic and nano particle diameter respectively. For nano wire[39] it is $\frac{8d}{3l}$ where d is nano particle diameter and l is atomic diameter. Similarly for nano filmand Disk like shape$\frac{N}{n}$ value is$\frac{4d}{3h}$ and $\frac{4}{3}$ d $(\frac{1}{h} + \frac{2}{l})$ here d, h and l are the diameter of the atom, the height of the nano solid and diameter of the nano solid respectively.Limitation of this model is that, when the particle radius (r) is below 20 nm, the semi-empirical model fails.

2.15 Surface Phonon Instability Model

The Surface Phonon Instability Model (SPI), created in 1991 by Wavtelet[35], is used to calculate the melting point of nanoparticles with radii larger than (2-4 nm).The model for surface phonon instability is as follows:

$$T_m = T_{mb}\left(1 - \frac{\beta}{d}\right) \quad ...(18)$$

Here T_m and T_{mb} is themelting point of nano particle and bulk particle respectively, d is thediameter of the nano particle,β is a Constant relating to atomic spacing.β depends upon temperature of the bulk materials temperature and energy intrinsic defect.

Limitation of the surface phonon instability model is that it is based on the idea that the mean phonon frequency varies according to the defect. The surface of the nanoparticle is assumed to be the same as the defect in the SPI model. Surface atoms are essential for calculating the melting depletion of materials with decreasing grain sizes.

3 Results and Discussion

Using the Gibbs-Thomson equation, LDM, and SPI, the melting point depression of Si and Zn nanoparticles have been computed by Seema et al.[40]. It is observed that when the particle size reduces, the Zn nanoparticle's melting temperature drops. For smaller nanoparticle sizes, there is a good match

between the experimental value from the literature and the values derived from the surface phonon instability model. Font et al.[41]useddistinct models to display a comparison between the particle radius and the experimentally determined melt temperature for gold. The melting point depression in nickel as a function of size has been predicted using a number of thermodynamic models. Teijlingen *et al.*[42] data casts doubt on these models' accuracy and demonstrates that the liquid nucleation and growth model fits the experimental data the best. Also Seema *et al.*[43] have determined the shape-based melting temperature depression of Ag nanoparticles using the semi-empirical model.

Fig. 8- displays the melting point depression for lead nanoparticles computed using the SPI model, LDM, and Gibbs-Thomson equation and compared with the published experimental value. It is evident from Fig.8-that the melting point determined by the Liquid Drop model is quite similar to the experiment value documented in the literature. The experimental value and the values determined by the Gibbs-Thomson equation and SPI are not the same.

Figure 9 It is found that the melting temperature of Pb nanoparticles is clearly based on the dimension of a nanoparticle. Since there have no experimental data on shape dependent melting behavior of nanoparticles in the Pb system in the literature, so there is no comparison with experimental values[44] has been made. From the results, it is concluded that the melting temperature is the maximum for Pb thin films and the minimum for tetrahedral-shaped Pb nanoparticles. The melting temperatures of all the other shapes that were taken into consideration for this study fall between those of thin films and tetrahedral-shaped nanoparticles. For the calculations, a straightforward model with accessible parameters is favoured among the several models for the melting point depression. The published data on several melting models is compared in Table 1.

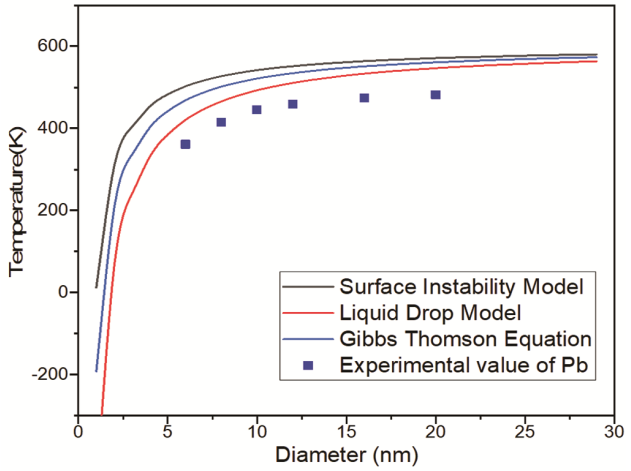

Fig. 8 — Pb melting point depression compared to experimental data using different melting models

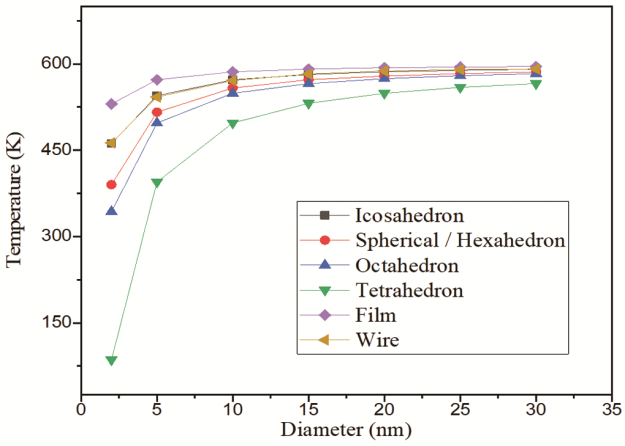

Fig. 9 — shows how the melting temperature of variously shaped Pb nanoalloys varies

Table 1 — Comparison of the literature data on different melting models

Alloy Systems	Type of nano phase diagram	Experimental/ Mathematical model used	Radius of the particle (nm)	Conclusions / Findings	Ref.
Au-Cu	Isomorphous	Regular solution model	4	Congruent melting shift to the lower temperature	45
Ag-Au	Isomorphous	CALPHAD method	100, 50, 20, 10 and 5	Decreases the melting temperature of the components	46
Au-Si, Cu-Pb, Bi-Cu,	Eutectic (Au-Si), Isomorphous (Cu-Pb) (Bi-Cu)	CALPHAD method	20, 10 and 5	Liquid phase region becomes enlarged	47
Ag-Cu	Eutectic	Differential Scanning Calorimetric, Transmission Electron Microscopy	20	Impulsive partition between Ag and Cu nanoparticles is produced.	48

(*Contd.*)

Table 1 — Comparison of the literature data on different melting models (*Contd*.)

Alloy Systems	Type of nano phase diagram	Experimental/ Mathematical model used	Radius of the particle (nm)	Conclusions / Findings	Ref.
Ag-Co	Isomorphous	Monte Carlo simulation And molecular dynamic simulation	10, 6, 4 and 2	Surface segregation of Ag-Co alloy is obtained with Co and Ag rich side.	49
Ag-Pd	Isomorphous	Molecular dynamic simulation	1.75, 1.45 and 1.25	Ag-liquidus Pd's and solidus curves get flatter the larger the cluster gets.	50
Ag-Sn	Eutectic	CALPHAD method	20	Decrease the eutectic temperature of the component	51
Co-Pt	Isomorphous	Tight-binding Ising model and Monte carlo simulation	1.5, 1 and 0.5	Surface segregation and core ordering Co-Ptnanoalloys are produced	52, 53
Cr-Mo	Isomorphous	Bond energy model	10	As particle size decreases, entropy, enthalpy, and heat of formation reduces.	54
Ni-Cu	Isomorphous	CALPHAD method, TEM, and DSC	10 and 5	Ni-Cu nanoparticles are prepared by wet synthesis of precursors and melting temperature reduces with the decrease of the size	55
Ni-Pd, Ni-Pt, Ni-Ir Ni-Rh	Isomorphous	Regular solution model	10 and 4	When the size is reduced Ni-Pt Ni-Rh and Ni-Pd show congruent melting but for Ni-Ir there is no congruent melting.	56
Ni-C	Eutectic	Monte Carlo simulation	10	Decrease the eutectic temperature of the component obtained.	57
Sn-Ag	Eutectic	CALPHAD method and Transmission Electron Microscopes	40	Surface tension affects the phase stability of Sn-Ag but not eutectic temperature or concentration.	58
In-Sb-	Eutectic	CALPHAD method and DFT calculation	80, 10 and 5	Eutectic temperature, eutectic composition, solidus and liquidus curves decrease.	59
Pt-Pd	Isomorphous	CALPHAD method	50, 20, 10 and 5	With a reduction in particle size, melting enthalpy and catalytic activation energy decline.	60 61
Pt-Rh	Isomorphous	Bond Order Simulation	3.9, 2.15and 1.55	Improves the orderly phases' stability when size reduces.	62
Si-Ge	Isomorphous	Regular solution model	5 and 2.5	Si and Ge's melting temperatures decreases as particle size decreases.	63
Bi-Sn	Eutectic	Transmission Electron Microscopes	15	Surface energy decreases when solute concentration increases	64

4 Conclusion

Given the vast array of applications for nanomaterials, it is imperative to compute the lowering of the melting point and comprehend the mechanism involved in the melting of nanoparticles.The melting point is lowered in relation to the bulk in melting models that take into consideration the material's finite size. The melting point of nanomaterials can be ascertained using a variety of thermodynamic and mathematical techniques, while keeping the bulk thermodynamic parameter values unchanged. It has been shown that the different melting behaviours of nanoparticles are what explain the different differences in melting temperatures. The goal of the current study is to analyse several melting models in order to establish the melting point depression as a function of nanoparticle size, taking into account the significance of having thermodynamic information on nanoparticles and nano alloy systems available. These models are quite flexible and useful for understanding the melting of different shaped nanoparticles. These thermodynamic models are useful in understanding the size-dependent melting of intermediate-sized nanoparticles.

References

1 Sun J & Simon S L, *Thermochimica Acta,* 463 (2007) 32.
2 Tokonami S, Morita N, Takasaki K & Toshima N, *J Phys Chem C,* 114 (2010) 10336.

3 Krajczewski J, Kolataj K & Kudelski A, *Appl Surf Sci,* 388 (2016) 624.
4 Zheng D, Hu C, Gan T, Dang X & Hu S, *Sensors Actuators B Chem,* 148 (2010) 247.
5 He H, Xu X, Wu H & Jin Y, *Mater,* 24 (2012) 1736.
6 Tabatabaei S, Kumar A, Ardebili H, Loos P J & Ajayan P M, *Microelectron Reliab,* 52 (2012) 2685.
7 Jiang H, Moon K S & Wong C P, *Microelectron Reliab,* 53 (2013) 1968.
8 Nezar H K, Basha T A & Gaber E E, *A Rev Membranes,* 5 (2023) 537.
9 Samikannu P, Ranjith K D, Kung-Yuh C & Tae H O, *J Indus Eng Chem,* 123 (2023) 402.
10 Qi W H & Wang M P, *J Mat Sci Lett, 21 (2002) 1743.*
11 Jones J E, *Jones Proc Royal Soc A: Math Phys Eng Sci,* 106 (1924) 463.
12 Lindemann F A, *Z Phys,* 11 (1910) 609.
13 Nanda K K, Sahu S N & Behera S N, *Phys Rev A,* 66 (2002) 013208.
14 Fedorov A V & Shulgin A V, *Combustion, Explosion Shock Waves,* 47 (2011) 147.
15 Zhu J, Fu Q, Xue Y & Cui Z, *Mater Chem Phys,* 192 (2017) 22.
16 Pawlow P, *Z Phys Chem,* 65 (1909) 545.
17 Reiss H, Wilson I B, *J Colloid Sci,* 3 (1948) 551.
18 Ubbelohde A R, *The Molten State of Matter Wiley:* New York, 1978.
19 Sakai H, *Surf Sci*, 351 (1996) 285.
20 Sun C Q, Wang Y, Tay B K, Li S, Huang H & Zhang Y B, *J Phys Chem B*, 106 (2002) 10701.
21 Guenther G & Guillon O, *J Mater Sci*, 49 (2014) 7915.
22 Lee J, Tanaka T, Lee J & Mori H, *Computer Coupling Phase Diagram Thermochemistry,* 31 (2007) 105.
23 Couchman P R & Jesser W A*, Nature,* 269 (1977) 481.
24 Reiss H, Mirabel P & Whetten R L, *J Phys Chem,* 92 (1988) 7241.
25 Richard R, Vanfleet & Mochel J M, *Surf Sci*, 341 (1995) 40.
26 Buffat P & Borel J P, *Phys Rev A*, 13 (1976) 2287.
27 Sun C Q, HL B, Li S, Tay B K & Jiang E Y, *Acta Mater*, 52 (2004) 501.
28 Sun C Q, *Prog Solid State Chem,* 35 (2006) 1.
29 Zhu J, Fu Q, Xue Y & Cui Z, *J Mater Sci,* 51 (22016) 4462.
30 Nanda K K, *Pramana,* 72 (2009) 617.
31 Reiss H & Wilson I B, *J Colloid Sci,* 3 (1948) 551.
32 Curzon A, University of London, London (1959).
33 Rie E, *J Phys Chem*, 104 (1923) 354.
34 Xiao S, Hu W & Yang J, *J Chem Phys,* 125 (2006) 184504.
35 Wautelet M, *J Phys D: Appl Phys,* 24 (1991) 343.
36 Johnson C A, *Surf Sci,* 3 (1965) 429.
37 Bhatt S & Kumar M, *J Phys Chem Solid,* 106 (2017) 112.
38 Gupta S K, Talati M & Jha P K, *Mater Sci Forum*, 570 (2008) 132.
39 Qi W H, *Physica B,* 368 (2005) 46.
40 Seema, Sharma A, Kashyap S, Zaidi B & Shekhar C, *J Nanoparticle Res,* 24 (2022) 107.
41 Font F & Myers T G, *J Nanoparticle Res,* 15 (2013) 12.
42 Van T A, Davis S A & Hall S R, *Nanoscale Adv,* (2020).
43 Seema, Yadav P, Kashyap S, Shekhar C, *J Nanoparticle Res,* 26 (2024) 160.
44 Skripov V P, KoverdaV P & Skokov V N, *Phys Status Solidi A,* 66 (1981).
45 Guisbiers G, Rosales S M, Khanal S, Zepeda F R, Whetten R L & Yacaman M J,*Nano Letter's*, 14 (2014) 6718.
46 Park J & Lee J, *Calphad,* 32 (2008) 135.
47 Tanaka T, *Mater Sci Forum*, 653 (2010) 55.
48 Sopousek J, Pinkas J, Brod P, Bursik J, Vykoukal V, Skoda D, Styskalik A, Zobac O, Vrestal J, Hrdlicka A & Simbera J, *J Nanomater,* (2014) 1.
49 Zheng Z, Fischer A & Cheng D, *Nanotechnology*, 27 (2016) 115702.
50 Kim D, Kim H, Ryu J H & Lee H M, *Phys Chem Chem Phys,* 11 (2009) 5079.
51 Sim K & Lee J, *J Alloys Compd,* 590 (2014) 140.
52 Lopes A, Treglia G, Mottet C & Legrand B, *Phys Rev B*, 91 (2015) 035407.
53 Qi W, Li Y, Xiong S & Lee S T, *Nano Micro Small,* 6 (2010) 1996.
54 W Qi, *Accounts Chem Res,* 49 (2016) 1587.
55 Sopousek J, Vrestal J, Pinkas J, Broz P, Bursik J, Styskalik A, Skoda D, Zobac O & Lee J, *Calphad,* 45 (2014) 33.
56 Guisbiers G, Perez R M, Diaz L B, Salazar J V & Yacaman M J, *The J Phys Chem C,* 121 (2017) 6930.
57 Magnin Y, Zappelli A, Amara H, Ducastelle F & Bichara C, *Phys Rev Lett,* 115 (2015) 205502.
58 Sopousek J, Vrestal J, Zemanova A & Bursik J, *J Mining Metal Sec B: Metal,* 48 (2012) 419.
59 Ghasemi M, Zanolli Z, Stankovski M & Johansson J, *Nanoscale*, 7 (2015) 17387.
60 Mendoza R & Guisbiers G, *Nanotechnology,* 30 (2019) 305702.
61 Guisbiers G, Abudukelimu G & Hourlier D, *Nanoscale Res Lett,* 6 (2011) 396.
62 Pohl J, Stahl C & Albe K, *Beilstein J Nanotechnol,* 3 (2012) 1.
63 Jiang Q & Yang C, *Current Nanosc*, 4 (2008) 179.
64 Dahan Y, Makov G & Shneck R Z, *Calphal,* 53 (2016) 136.